



Published in final edited form as:

J Immunol. 2010 June 15; 184(12): 7207–7218. doi:10.4049/jimmunol.0903487.

The prostaglandin E₂ EP4 receptor exerts anti-inflammatory effects in brain innate immunity

Ju Shi^{*}, Jenny Johansson^{*}, Nathaniel S. Woodling^{*}, Qian Wang^{*}, Thomas J. Montine[†], and Katrin Andreasson^{*}

^{*}Department of Neurology and Neurological Sciences, Stanford University School of Medicine, Stanford, CA 94305

[†]Department of Pathology, University of Washington, Seattle, WA 98104

Abstract

Peripheral inflammation leads to immune responses in brain characterized by microglial activation, elaboration of pro-inflammatory cytokines and reactive oxygen species, and secondary neuronal injury. The inducible cyclooxygenase COX-2 mediates a significant component of this response in brain via downstream pro-inflammatory prostaglandin signaling. Here, we investigated the function of the PGE₂ EP4 receptor in the central nervous system (CNS) innate immune response to the bacterial endotoxin lipopolysaccharide (LPS). We report that PGE₂ EP4 signaling mediates an anti-inflammatory effect in brain by blocking LPS-induced pro-inflammatory gene expression in mice. This was associated in cultured murine microglial cells with decreased Akt and IKK phosphorylation and decreased nuclear translocation of p65 and p50 NF-kappaB subunits. In vivo, conditional deletion of EP4 in macrophages and microglia increased lipid peroxidation and pro-inflammatory gene expression in brain and in isolated adult microglia following peripheral LPS administration. Conversely, EP4 selective agonist decreased LPS-induced pro-inflammatory gene expression in hippocampus and in isolated adult microglia. In plasma, EP4 agonist significantly reduced levels of pro-inflammatory cytokines and chemokines, indicating that peripheral EP4 activation protects the brain from systemic inflammation. The innate immune response is an important component of disease progression in a number of neurodegenerative disorders such as Alzheimer's disease, Parkinson's disease, and amyotrophic lateral sclerosis. In addition, recent studies demonstrate adverse vascular effects with chronic administration of COX-2 inhibitors, indicating that specific prostaglandin signaling pathways may be protective in vascular function. This study supports an analogous and beneficial effect of PGE₂ EP4 receptor signaling in suppressing brain inflammation.

Keywords

neuroinflammation; COX-2; PGE₂; EP4 receptor; lipopolysaccharide; innate immunity

Introduction

The inflammatory response in the central nervous system (CNS) plays a critical role in the pathogenesis of many neurodegenerative diseases including Alzheimer's disease (AD), Parkinson's disease (PD), and amyotrophic lateral sclerosis (ALS), and contributes to aging in brain. Participating in the neuroinflammatory response are the innate and adaptive

immune responses, which mediate intrinsic phagocytic and lymphocyte-mediated responses, respectively. Significant insight has been gained into the role of inflammation in neurodegeneration in AD, PD, and ALS from studies of innate immunity because of considerable overlap in cellular and molecular inflammatory mechanisms (1-7). A well-studied model of innate immunity in brain involves systemic administration of the bacterial endotoxin lipopolysaccharide (LPS). The peripheral immune response to LPS can be transmitted to brain parenchyma in several ways: by direct effects on circumventricular organs or perivascular macrophages, stimulation of vagal afferents, direct transport of cytokines into brain, and transduction of serum immune responses to parenchyma via endothelial cells. The resultant CNS innate immune response is characterized by activation of microglial cells and generation of neurotoxic reactive oxygen species, cytokines, and proteases that lead to neuronal and synaptic injury and behavioral deficits (6, 8-11).

A major participant in the neuroinflammatory process is the inducible isoform of cyclooxygenase, or COX-2, which elicits an injurious inflammatory response in many models of neurological disease (reviewed in (12-15)). COX-2 and the constitutively expressed isoform COX-1 catalyze the first committed step in the synthesis of the five prostaglandins, PGE₂, PGD₂, PGF_{2α}, PGI₂, and TXA₂, which in turn signal through distinct classes of G-protein coupled receptors (16, 17). Studies to understand the toxic effects of COX-2 in models of inflammation have accordingly focused on downstream prostaglandin signaling pathways, notably PGE₂ which signals through a class of four EP (for E-prostanoid) receptors, termed EP1-EP4 (reviewed in (18)). So far, studies indicate that the PGE₂ EP2 receptor mediates a significant neuroinflammatory response in vivo in a broad range of neurodegenerative models, including the LPS model of innate immunity (19), the APPSwe-PS1ΔE9 model of Familial AD (20), the G93ASOD model of Familial ALS (21), and the 1-methyl-4-phenyl-1,2,3,6-tetrahydropyridine (MPTP) model of PD (22). Interestingly, the function of EP2 signaling in brain is likely to be context-specific, as studies demonstrate a neuroprotective effect of EP2 signaling in models of glutamate toxicity and cerebral ischemia (23-28).

The PGE₂ EP4 receptor shares certain characteristics with the EP2 receptor in that it is positively coupled to cAMP and its expression is strongly induced in brain with systemic LPS administration (29). However, the function of the EP4 receptor in vivo in CNS innate inflammation is not known. Here we report that unlike the EP2 receptor, the EP4 receptor exerts significant anti-inflammatory effects in vitro and in vivo by suppressing the pro-inflammatory gene response in the LPS model of innate immunity, indicating that the PGE₂ EP4 receptor is likely to function as a beneficial prostaglandin receptor in vivo in CNS inflammatory diseases.

MATERIALS AND METHODS

Materials

Lipopolysaccharide (LPS, *Escherichia coli* O55: B5; Calbiochem, La Jolla, CA) was resuspended in sterile phosphate-buffered saline (PBS) at 1mg/ml and stored at -20°C. EP4 specific agonist AE1-329 {16-(3-methoxymethyl) phenyl-omega-tetranor-3,7-dithia prostaglandin E1} was a generous gift from Ono Pharmaceuticals Co., Osaka, Japan. Its selectivity for the EP4 receptor has been previously established (30, 31). H-89 was purchased from Biomol (Plymouth Meeting, PA). Cell culture media, supplements, and antibiotics were purchased from Invitrogen (Carlsbad, CA).

Animals

This study was conducted in accordance with the National Institutes of Health guidelines for the use of experimental animals and protocols were approved by the Institutional Animal Care and Use Committee. C57B6 EP4 floxed mice (32) were kindly provided by Drs. Richard and Matthew Breyer (Vanderbilt University School of Medicine, Nashville, TN), and C57B6 Cd11bCre mice (33) were kindly provided by Dr. G. Kollias (Alexander Fleming Biomedical Sciences Research Center, Vari, Greece) and Dr. Donald Cleveland (UCSD, San Diego, CA). All mice were housed in an environment controlled for lighting (12 hour light/dark cycle), temperature, and humidity, with food and water available ad libitum. Cd11bCre:EP4f/f and Cd11bCre:EP4+/+ mice were generated by serial crosses of C57B6 Cd11bCre and EP4f/f and EP4+/+ lines. Male Cd11bCre: EP4f/f and Cd11bCre: EP4+/+ mice were treated with either saline or LPS (5mg/kg intraperitoneally; n=5-8 per group, 13 months of age). 24 hours after injection, mice were euthanized and brain tissue was harvested and frozen at -80°C . For pharmacological experiments, C57B6 male mice (Jackson Laboratories, Bar Harbor, ME; n=7 or 8 per group) received an injection of saline or LPS (5mg/kg, i.p. (6)) +/- vehicle or AE1-329 (300 $\mu\text{g}/\text{kg}$ subcutaneously (34)). Mice were euthanized 6 hours later, and brain tissue was harvested and frozen at -80°C . For collection of plasma, C57B6 male mice (n=5 per group) received an injection of saline or LPS (5mg/kg, i.p.) +/- AE1-329 (300 $\mu\text{g}/\text{kg}$ s.c.) or vehicle. Mice were deeply anesthetized with isoflurane at 3h and blood was collected in a 1-ml syringe pre-coated with EDTA (250mM) and placed in EDTA coated tubes. Plasma was collected after centrifugation at 1000 $\times g$ for 10 min at 4°C and frozen at -80°C .

Cell culture

Murine microglial-like BV-2 cells were grown in DMEM medium supplemented with 10% heat-inactivated fetal bovine serum (HyClone, Logan, Utah) and 100 units/ml each of penicillin and streptomycin and were maintained at 37°C in a humidified atmosphere containing 5% CO_2 . For primary microglial cultures, cerebral cortices were isolated from postnatal day 2 Sprague-Dawley rat pups obtained from Charles River Laboratories International, Inc. (Davis, CA) Tissues were minced and incubated in 0.25% trypsin-EDTA, mechanically triturated in DMEM/F-12 with 10% FBS, and plated on poly-L-lysine-coated 75ml flasks. Cultures were maintained for 14 days with media changes every 4 days. Microglial cells were isolated by shaking flasks at 200 rpm in a Lab-LineTM Incubator-Shaker for 6 h. The purity of microglial cultures was confirmed with immunostaining for Iba1 and was >95% pure. BV-2 cells were seeded onto 6-well or 24-well plates and allowed to grow to 80–90% confluence. Primary microglia were seeded onto 24 well plates at 5×10^5 cells per ml.

Quantitative Real Time PCR (qPCR)

qPCR was carried out as previously described (21). Briefly, total RNA was isolated using Trizol reagent (Invitrogen, Carlsbad, CA), treated with DNase (Invitrogen), and the reaction was terminated by heating at 65°C for 10 minutes. First strand cDNA synthesis was performed with 1.5 μg of total RNA, 4 units of Omniscript enzyme (Qiagen, Valencia, CA) and 0.25 μg of random primer in a reaction volume of 20 μl at 37°C for 1 hour. Reverse transcribed cDNA was diluted 1:20 in RNase free ddH₂O for subsequent RT-PCR. The mRNA level for each target gene was quantified by SYBR Green-based qPCR using the QuantiTect SYBR Green PCR kit (Qiagen). Melting curve analysis confirmed the specificity of each reaction. Forward and reverse oligonucleotide primers for interleukin-6 (IL-6), interleukin-1 β (IL-1 β), tumor necrosis factor- α (TNF- α), inducible nitric oxide synthase (iNOS), COX-2, NADPH subunits gp91^{phox}, p67^{phox}, p47^{phox}, and interleukin-10 (IL-10) (IDT Integrated DNA Technologies, Coralville, IA) are listed in Supplementary Table 1. The reaction was performed using 5 μl of cDNA, 0.25-0.5 μM of primer, and 2x SYBR

Green Super Mix (Qiagen) with a final volume of 25 μ L. Quantification was performed using the standard curve method. Gene expression level was normalized to 18S RNA, and relative mRNA expression is presented relative to control. Samples without reverse transcriptase served as the negative control. PCR assays were performed using the PTC-200 Real Time PCR System (MJ Research). Experiments were repeated in triplicate.

Immunostaining

Free-floating 40 μ m coronal brain sections through hippocampus were generated and processed for immunostaining as previously described (20). The following primary antibodies were used: anti-EP4 (1/1000; Cayman Chemicals, Ann Arbor, MI) and anti-Iba1 (1/500; Wako, Richmond, VA). Secondary antibodies and detection reagents included donkey anti-mouse Alexa 555, anti-rabbit Alexa 486, and Zenon 555 for detection of Iba1 (Molecular Probes, Eugene, OR). Specific staining of the EP4 antibody was confirmed using blocking peptide and no primary antibody in control experiments. Images were acquired by sequential scanning using the Leica TCS SPE confocal system and DM 5500 Q microscope (Leica Microsystems, Mannheim, Germany) with laser lines 405, 488 and 532 nm. Sections corresponding to 6 μ M were selected and equally processed in Leica LAS AF (Leica Microsystems) and collapsed stacks were obtained with MetaMorph software (Molecular Devices, Sunnyvale, CA).

Nuclear extract preparation

Nuclear and cytoplasmic fractions of BV-2 cells were prepared at several time points after treatment (0-120 minutes) using the nuclear extract kit from Active Motif (Carlsbad, CA). Briefly, cells were washed, collected in ice-cold PBS in the presence of phosphatase inhibitors, and centrifuged at 300 $\times g$ for 5 min at 4°C. Cell pellets were resuspended in hypotonic buffer, treated with detergent, and centrifuged at 14,000 $\times g$ for 30 sec at 4°C. After collection of the cytoplasmic fraction, nuclei were solubilized for 30 min in lysis buffer containing protease inhibitors. Lysates were centrifuged at 14,000 $\times g$ for 30 min at 4°C and supernatants were collected for NF- κ B studies. To prepare whole cell lysates for phospho-Akt and phospho-IKK studies, cells were washed in ice-cold PBS and lysed in 20mM Tris-HCl, pH 7.5, 150mM NaCl, 1mM Na₂EDTA, 1mM EGTA, 1% Triton, 2.5 mM sodium pyrophosphate, 1mM β -glycerophosphate, 1mM orthovanadate, 1 μ g/ml leupeptin and 1mM PMSF. Lysates were sonicated for 5 seconds, centrifuged at 14,000 $\times g$ for 10 min at 4°C and supernatants were collected for phospho-Akt and phospho-IKK studies. All protein concentrations were determined using the Bradford protein assay.

Western blot analysis

Protein (20 μ g per lane) was fractionated using 12% SDS-PAGE and electrophoretically transferred to PVDF membranes (Bio-Rad, Hercules, CA). For phospho-Akt/Akt and phospho-IKK/IKK studies, membranes were probed with anti phospho-Ser473 Akt antibody or anti-phospho-IKK antibody (1:1000, Cell signaling, Beverly, MA) and anti-Akt and anti-IKK antibodies (1:1000; Cell Signaling). For NF- κ B nuclear translocation studies, membranes were probed with anti-NF- κ B p105/p50 antibody (1:5000, Abcom, Cambridge, MA) or anti-NF- κ B p65 antibody (1:300, Santa Cruz Biotechnology). Loading controls included anti-actin antibody (1:10,000, Santa Cruz Biotechnology, Inc. Santa Cruz, CA) for cytosolic fractions and anti-lamin B1 antibody (1:10,000, Abcom, Cambridge, MA) for nuclear fractions. Immunoreactivity was detected using either sheep anti-rabbit or sheep anti-mouse HRP-conjugated secondary antibody (Amersham Biosciences, Arlington Heights, IL), followed by enhanced chemiluminescence (Pierce). Autoradiographic signals were quantified using NIH Image. Experiments were repeated in triplicate.

Griess assay

NOS activity was measured using the Griess assay to measure nitrite production (Promega, Madison, WI). BV-2 cells were plated at 5×10^4 cells/well in 24-well plates, allowed to reach 90% confluence, and incubated +/- LPS (10ng/ml) +/- AE1-329 (1nM-1 μ M) or vehicle for 24h. 50 μ l cell culture medium and nitrite standards (0 to 100nM) were transferred to a 96-well plate and mixed with 50 μ l sulphanilamide solution and 50 μ l NED solution. After a 10 min incubation at room temperature, absorbance was read at 530 nm on a SpectraMax M5 plate reader (Molecular Devices, Sunnyvale, CA). Experiments were repeated in triplicate.

PKA activity assay

PKA activity was determined using the PKA kinase activity assay kit (Assay designs, Ann Arbor, Michigan). Cells were harvested 3 minutes after stimulation, and ELISA was carried out according to the manufacturer's instructions. Kinase activity was calculated as (sample absorbance – blank absorbance)/ μ g protein and normalized to the average value of vehicle.

ELISA

Measurements of phospho-Akt and total Akt were determined using the PathScan phospho-Akt (Thr308) and total Akt1 ELISA kits (Cell Signaling Technology, Danvers, MA). BV-2 cells were harvested in cell lysis buffer 1 hr after stimulation (20mM Tris pH7.5, 150 mM NaCl, 1mM EDTA, 1mM EGTA, 1% TritonX-100, 2.5mM sodium pyrophosphate, 1mM β -glycerophosphate, 1mM Na_3VO_4 , 1 μ g/ml leupeptin), and ELISA was carried out according to the manufacturer's instructions. The ratio of phospho-Akt to total Akt was used for statistical analysis.

Immunocytochemical quantification of NF- κ B-p65 nuclear translocation

BV-2 cells were seeded on poly-L-Lysine coated glass coverslips and were maintained in culture for at least 24 hours before treatment with LPS +/-AE1-329. After one hour of treatment, cells were fixed with 4% paraformaldehyde and processed for immunocytochemistry using established protocols. NF- κ B cellular localization was detected using rabbit anti-NF- κ B p65 antibody (1:200, Santa Cruz Biotechnology) and Cy3-conjugated donkey anti-rabbit secondary antibody (Jackson ImmunoResearch Laboratories, West Grove, PA). Nuclei were visualized using Hoechst 33258 dye (MP Biomedicals, Solon, OH). Images were acquired using a Nikon Eclipse E600 microscope (Nikon Instruments, Melville, NY) and a Hamamatsu Orca-ER digital camera (Hamamatsu Photonics, Bridgewater, NJ). For quantification of nuclear NF- κ B p65 levels, images were analyzed using the measurements module of Volocity 4.3.2 image analysis software (Improvision Inc., Waltham, MA). To define nuclei, a measurements protocol found all areas of the image where the Hoechst signal was above a defined threshold. Further steps separated touching nuclei into individual objects, excluded objects smaller than 30 μm^2 , and excluded objects touching the edge of the image. The program then reported the average intensity of the NF- κ B p65 (Cy3) signal for each nucleus. For data quantification, each data point represented the average NF- κ B p65 signal from the nuclei in one field of view (>100 cells).

Measurement of F2-isoprostanes and F4-neuroprostanes

Cd11b:EP4f/f and control Cd11bCre:EP4+/+ cerebral cortices were examined for levels of lipid peroxidation by assaying for F2-isoprostanes (F2-IsoPs), which are free radical-generated isomers of prostaglandin $\text{PGF}_{2\alpha}$ in neuronal and non-neuronal cells, and F4-neuroprostanes (F4-NeuroPs), which are neuron-specific products of docosohexanoic acid oxidation using gas chromatography with negative ion chemical ionization mass spectrometry as described previously (20).

Isolation of adult microglia from mouse brain

Adult microglial cell isolation was carried according to the methods of Cardona et al.(35) and cells were processed for RNA isolation or flow cytometry. Mice were deeply anesthetized and perfused with 30 ml ice cold 0.9% saline, and brains were harvested and washed in ice-cold PBS, and individually homogenized using a dounce tissue homogenizer in 4 ml digestion cocktail (RPMI 1640 with 300U/ml collagenase) and incubated for 45 min at 37°C. Collagenase activity was stopped with the addition of 20ml of HBSS with 2% fetal bovine serum and 2mM EDTA. The suspension was triturated and passed through a 100 µm cell strainer (BD Falcon, Bedford, MA) and centrifuged at 300×g for 10 min at 4°C. The cell pellet was resuspended in 3.3 ml 75% isotonic Percoll (Sigma, St Louis, MO), overlaid with 5ml 25% isotonic Percoll and 3 ml ice-cold PBS, and spun at 800×g for 60 min at 4°C without brakes. After centrifugation, cells at the interphase between the 75% and 25% Percoll layers were carefully collected and diluted in 10ml PBS with 0.5% FBS and 2mM EDTA and centrifuged at 300×g for 10 min at 4°C. Yields of $\sim 2.0 \times 10^5$ microglial cells per brain were obtained, consistent with published studies (36), yielding ~ 200 ng of microglial RNA per brain. Purity of the microglial preparation was determined in separate experiments by labeling $\sim 10^5$ cells/ml with phycoerythrin (PE)-conjugated hamster anti-mouse CD11b or IgG isotype control (1:100; eBioscience, San Diego, CA) for 30 minutes on ice. Cells were then washed with PBS and fixed (BD, Biosciences, San Diego, CA). Flow cytometry was performed on a LSR II (BD Biosciences), and data analyzed with FlowJo 7.2.2 software. Cells obtained by density gradient centrifugation were 90.39% Cd11b positive (Supplementary Figure 3A). In separate experiments, magnetic beads conjugated to anti-mouse Cd11b antibody (Miltenyi Biotec, Bergisch Gladbach, Germany) were used to further purify Cd11b positive microglia as described in deHaas et al. (36). Cells at the Percoll interphase were resuspended in 90 µl ice-cold bead buffer (PBS with 0.5% FBS and 2mM EDTA, pH7.2) and incubated with 10 µl anti-mouse CD11b-coated beads at 4°C for 15 min and then rinsed in bead buffer. Cells were pelleted at 300 x g for 10 min at 4°C and separated using a magnetic MACS Cell Separation column (Miltenyi Biotec). Flow cytometry analysis demonstrated that microglia were 97.6% Cd11b positive following this step, however cell yield was substantially decreased (Supplementary Figure 3B). Therefore, cells purified by density centrifugation were used for RNA preparation.

Plasma multi-analyte analysis

Plasma was analyzed using the Rodent MAP™ Antigens, Version 2.0 multi-analyte profile (Rules Based Medicine, Austin, TX) that screens a total of 59 blood secreted proteins using multiplex fluorescent immunoassay.

Statistical Analysis

Data are presented as mean \pm standard error of the mean and analyzed using analysis of variance or Student's *t* test. Prism software (GraphPad Software, Inc. San Diego, CA) was used for statistical analyses. Data for Griess assays and quantitative Western analyses were analyzed using one-way or two-way ANOVA, followed by Newman-Keuls multiple comparison or Bonferroni posttest analysis, respectively. For plasma multi-analyte analysis, the concentrations of the 15 plasma proteins that reached statistical significance between LPS+vehicle versus LPS+AE1-329 cohorts were transformed to relative concentrations (Median Z-score). Cluster analysis (Gene Cluster3.0, University of Tokyo, Tokyo and Java TreeView 1.0.13, Alok Saldanda, CA) produced a separation of samples according to treatment group and protein levels in plasma. For all data, a probability level of $p < 0.05$ was considered to be statistically significant.

RESULTS

Expression of EP4 receptors in microglia

We first determined whether PGE₂ EP4 receptor is expressed in BV-2 cells and in primary cultured microglia and whether it is regulated in response to LPS stimulation. The murine microglial BV-2 cell line exhibits phenotypic and functional properties of microglial cells and has been widely used to model microglial responses (37), in large part because of the limited yields obtained with primary microglial cultures. Quantitative reverse transcriptase polymerase chain reaction (qPCR) demonstrated that EP4 messenger RNA (mRNA) was expressed in both BV-2 and primary cultured microglia (Figure 1A and B). Following LPS stimulation (10ng/ml), there was a rapid increase in EP4 mRNA at 6 hours in BV-2 cells ($p < 0.01$; Figure 1A). A time course in primary microglia showed a strong induction of mRNA peaking at 3 hours (25.25 ± 2.91 fold increase of relative mRNA expression compared with vehicle-treated cells at 3 hours; ANOVA $p < 0.0001$; Figure 1B). These data indicate that the EP4 receptor is dynamically upregulated in microglia by LPS. In hippocampus from vehicle and LPS stimulated mice, EP4 mRNA was also dynamically upregulated at 6 hours, returning to baseline by 24 hours ($p < 0.05$; Figure 1C). Confocal microscopy at 6 hours after stimulation with either vehicle or LPS demonstrated EP4 receptor localization in Iba1 positive microglia in hippocampus in a punctate perinuclear area (arrows, Figure 1D) in both saline and LPS treated mice. Microglia underwent morphological changes by 6 hours after LPS as evidenced by induction of cytosolic Iba1 staining and thickening of microglial processes (Supplementary Figure 1). The punctate perinuclear localization of EP4, as well that of other EP receptors to perinuclear areas, has been previously described in other cell types (38-40).

EP4 receptor activation attenuates LPS-induced proinflammatory gene expression in BV-2 cells and primary microglia

Inflammatory stimuli such as LPS can activate microglia through the CD14/TLR4 receptor complex and induce the expression of pro-inflammatory enzymes and cytokines (2, 3). We tested whether pharmacologic activation of EP4 receptor with the selective EP4 agonist AE1-329 would alter LPS-induced inflammatory responses. BV-2 cells were treated with LPS (10ng/ml) in the presence or absence of the selective EP4 agonist AE1-329 (1 μ M) for 6h, and pro-inflammatory gene expression was measured using qPCR (Figure 2). As expected, LPS significantly induced expression of pro-inflammation enzymes COX-2, iNOS, and the NADPH oxidase subunit gp91^{phox} ($\#p < 0.001$; Figure 2A) as well as candidate pro-inflammatory cytokines including TNF- α , IL-6 and IL-1 β ($\#p < 0.001$; Figure 2B). However, co-stimulation with EP4 agonist significantly blunted the induction of these genes ($*p < 0.05$ for COX-2, iNOS and cytokines TNF α , IL-1 β , and IL-6; $**p < 0.01$ for gp91^{phox}). Conversely, co-stimulation with AE1-329 significantly induced expression of the anti-inflammatory IL-10 mRNA (Figure 2C; $*p < 0.05$). We further examined EP4 regulation of iNOS activity (Figure 2D). NO production was significantly elevated at 24 hours in BV-2 cells following LPS treatment (Figure 2D; $\#p < 0.001$). However, co-stimulation with AE1-329 dose-dependently reduced NO production (decreasing 68.9% from 21.76 μ M nitrite to 6.57 μ M with 10nM AE1-329; ANOVA $p < 0.001$, post hoc $p < 0.001$ for 1, 10, 100, and 1000nM AE1-329). Finally, co-stimulation of LPS treated primary microglia with AE1-329 at 3h also demonstrated a downregulation of pro-inflammatory gene expression (Figure 2E) and an upregulation of the anti-inflammatory IL-10. Taken together, these data indicate that EP4 exerts an anti-inflammatory effect in BV-2 cells and primary microglial cells by suppressing the induction of LPS-induced pro-inflammatory gene expression and increasing expression of anti-inflammatory IL-10.

EP4 receptor signaling involves PKA activation and reduction of Akt phosphorylation

Downstream signaling events for EP4, a G α -coupled receptor, were investigated in LPS treated BV-2 cells (Figure 3). Stimulation of BV-2 cells with AE1-329 or AE1-329 and LPS together significantly increased PKA activity, indicating that the EP4 receptor is positively coupled to cAMP and PKA activation in BV-2 cells. The increase in PKA activity from EP4 receptor signaling was blocked with the PKA inhibitor H89 at doses of 5 μ M and 10 μ M (Figure 3B).

In addition to its known G α s coupling to PKA, the EP4 receptor can signal via PI3K and Akt via a G α i subunit (41, 42). To further investigate whether EP4 signaling regulates PI3K/Akt pathway activity in LPS-stimulated BV-2 cells, levels of phospho-Akt were measured using quantitative Western analysis (phosphorylated Ser473 Akt; Figure 3C) and ELISA (phosphorylated Thr308 Akt; Figure 3D). Phosphorylation at both residues Ser473 and Thr308 is required for Akt activation. Quantitative Western demonstrated a significant attenuation of phospho-Ser473Akt signal in LPS treated BV-2 cells stimulated with EP4 agonist over 60 minutes ($p < 0.05$ for effect of AE1-329 and $p < 0.001$ for effect of time, see Figure 3 legend). ELISA of phospho-Thr308 Akt also demonstrated a significant decrease in LPS-treated cells at 60 minutes after stimulation with EP4 agonist ($p < 0.01$). Stimulation with EP4 agonist alone did not alter Akt phosphorylation in the absence of LPS. Taken together, these data indicate that EP4 receptor activation in LPS-treated BV-2 cells reduces Akt phosphorylation.

EP4 receptor activation attenuates LPS-induced IKK phosphorylation and decreases nuclear factor-kappaB (NF- κ B) nuclear translocation

We then investigated the anti-inflammatory signaling of EP4 downstream of PI3K/Akt in BV-2 cells. PI3K phosphorylation of Akt can regulate NF- κ B nuclear translocation through phosphorylation of the inhibitory I- κ B kinase complex (IKK). Phospho-Akt activates the IKK complex by phosphorylating serines on the IKK α and IKK β subunits (43-46) but see (47), and activated IKK phosphorylates I- κ B and targets it for degradation, allowing NF- κ B to translocate to the nucleus (48). Nuclear translocation of NF- κ B induces expression of many pro-inflammatory genes including COX-2, iNOS, TNF- α , IL-1 β , and IL-6. Because of the broad range of pro-inflammatory genes downregulated by EP4 signaling in microglial cells, we tested whether EP4 affected NF- κ B activation and nuclear translocation in LPS-stimulated BV-2 cells.

LPS stimulation induced the phosphorylation of IKK, but this was attenuated with co-stimulation with EP4 agonist (Figure 4A; $p < 0.05$ 2-way ANOVA). In addition, LPS treatment induced a time-dependent nuclear translocation of NF- κ B subunits p65 and p50, but co-stimulation with AE1-329 reduced levels of NF- κ B nuclear translocation (Figures 4B and 4C; $p < 0.01$ 2-way ANOVA for both p65 and p50) as compared to vehicle; moreover cytoplasmic levels of p65 and p50 were increased in LPS-treated cells stimulated with AE1-329 as compared to vehicle stimulated cells. Semi-quantitative measurements of p65 immunofluorescent signal also revealed an increase in nuclear translocation with LPS treatment (Figure 4D and E; $p < 0.001$) that was significantly attenuated with co-stimulation of EP4 receptor ($p < 0.01$). Therefore, EP4 receptor activation decreased LPS-induced phosphorylation of Akt and IKK, and decreased translocation of NF- κ B subunits p65 and p50 to the nucleus, providing a potential mechanism for its downregulation of pro-inflammatory genes.

Cd11bCre-mediated conditional deletion of EP4 receptor leads to increased LPS-induced pro-inflammatory gene expression and lipid peroxidation in brain

The *in vitro* data described above indicate an anti-inflammatory effect of EP4 signaling in BV-2 cells and primary microglia. To test this *in vivo*, we generated Cd11bCre:EP4^{+/+} and Cd11bCre:EP4^{f/f} mice where the EP4 receptor is selectively deleted in cells of monocytic lineage, including microglia and macrophages. From the *in vitro* experiments in Figure 2 demonstrating that EP4 receptor signaling suppresses pro-inflammatory gene expression, we hypothesized that conditional deletion of EP4 in microglia/macrophages would conversely lead to increased pro-inflammatory gene expression with LPS stimulation. In addition, increased pro-inflammatory protein expression and activity would likely lead to increased inflammatory oxidative stress, leading to increases in lipid peroxidation which can be reliably measured by 24 hours after LPS stimulation (19-21). We therefore examined a time point *in vivo* of 24 hours after peripheral administration of LPS in these mice.

Peripheral stimulation with LPS results in peripheral and CNS inflammatory responses (49, 50). Because this neuroinflammatory response can induce synaptic and neuronal injury and disrupt hippocampal-dependent memory, we examined pro-inflammatory gene expression in hippocampus in Cd11bCre:EP4^{f/f} mice and control Cd11bCre:EP4^{+/+} littermates treated with LPS (5 mg/kg *i.p.*; Figure 5). At 24 hours after LPS, there was no difference in pro-inflammatory gene expression between vehicle and LPS-treated wild-type mice, reflecting the documented resolution of the inflammatory response by that time point (49). However, in EP4 conditional knockout mice stimulated with LPS, expression of COX-2, TNF- α , IL-6, IL-1 β as well as subunits of the NADPH oxidase complex, including gp91^{phox}, p67^{phox}, and p47^{phox} were all significantly upregulated at 24 hours (Figure 5A, B). Levels of cerebral cortical lipid peroxidation showed no differences in levels of neuronal-specific F4 neuroprostanes, however levels of F2-isoprostanes were significantly higher in Cd11b:EP4^{f/f} cerebral cortices compared with Cd11b:EP4^{+/+} mice ($p < 0.05$). Arachidonic acid, a major component of membrane phospholipids in all brain cell types, is particularly vulnerable to free radical attack and its peroxidation is reflected in the F2-isoprostane measurements. These *in vivo* data complement the *in vitro* findings in cultured microglial cells, and indicate that EP4 functions in an anti-inflammatory manner *in vivo* in brain inflammation. However, in spite of the increased pro-inflammatory gene expression and lipid peroxidation, we did not observe overt differences in hippocampal microglial morphology between genotypes following LPS administration at 24 hours (Supplementary Figure 2).

Effect of EP4 agonist on LPS-induced innate immunity *in vivo*

In vitro stimulation of LPS-treated microglial BV-2 cells and primary microglia resulted in a broad downregulation of pro-inflammatory gene expression by 6 hours after stimulation (see Figure 2). To confirm a similar acute anti-inflammatory effect of EP4 signaling *in vivo*, we treated mice with LPS (5mg/kg, *i.p.*) with or without EP4 agonist AE1-329 (300 μ g/kg, *s.c.*; Figure 6) and examined mRNA expression at 6 hours, a similar time point to that used *in vitro*. As expected, LPS led to significant increases in hippocampal mRNA of pro-inflammatory cytokines TNF- α , IL-6, IL-1 β as well as COX-2, iNOS, and the NADPH oxidase subunits gp91^{phox}, p67^{phox}, and p47^{phox} genes (not shown) at 6 hours after LPS. Co-administration of EP4 agonist significantly attenuated LPS-induced COX-2, iNOS, TNF- α , IL-6, and IL-1 β mRNA levels in hippocampus; there was a trend toward decreased expression of NADPH oxidase subunit gp91^{phox}, p67^{phox}, and p47^{phox} (not shown). Thus, peripheral administration of a selective EP4 agonist significantly blunted the CNS inflammatory response to systemic LPS in a time course similar to *in vitro* studies in BV-2 cells and primary microglia. Microglial morphological changes in response to LPS appeared modestly decreased with co-administration of EP4 agonist (Supplementary Figure 1).

EP4 signaling regulates inflammatory gene expression in microglia isolated from adult brain

To further confirm that EP4 signaling regulated expression of inflammatory genes in brain microglia *in vivo*, microglia were acutely isolated from wild type adult mice stimulated +/- LPS +/- EP4 agonist (Figure 7A) and from Cd11bCre:EP4f/f and Cd11bCre:EP4+/+ mice stimulated +/- LPS (Figure 7B). For pharmacological experiments (Figure 7A), 2-3 mo C57B6 male mice (n=6-8 per group) received an injection of saline or LPS (5mg/kg, i.p.) +/- vehicle or AE1-329 (300µg/kg subcutaneously) and microglia were harvested for RNA isolation at 6 hours, similar to the time point used for post-natal microglia (see Figure 2E). Administration of LPS led to significant increases in microglial COX-2, iNOS, IL-6, TNF- α , and gp91^{phox} that were significantly reduced with co-administration of EP4 agonist. Conversely, genetic experiments examining microglia isolated from adult Cd11bCre:EP4+/+ and Cd11bCre:EP4f/f C57B6 mice +/- LPS demonstrated that the normal downregulation of pro-inflammatory gene expression at 24 hours in Cd11bCre:EP4+/+ mice was blocked in the Cd11bCre:EP4f/f mice. In this experiment, we also tested a 6 hour time point, which did not show differences in inflammatory gene induction between genotypes. Thus, microglial EP4 deletion results in persistently elevated inflammatory gene expression at 24 hours, confirming similar findings in whole hippocampal mRNA (see Figure 5).

EP4 receptor activation attenuates plasma cytokine levels induced in response to LPS

The innate immune response in brain to systemic inflammation can occur as a direct response in brain or as a peripheral-to-central immune response, in which serum cytokines either are transported across the blood-brain barrier or act on endothelium to transduce the inflammatory response to brain parenchyma. IL-6, IL-1 β , and TNF α are generated as part of peripheral inflammation by macrophages, and are well-documented effectors of peripheral-to-central immune responses where peripheral inflammatory signals lead to expression of cytokines in brain. In the case of the EP4 conditional knockout (cKO), where EP4 is deleted in peripheral macrophages as well as CNS microglia, the anti-inflammatory effects of EP4 may be mediated by brain microglia, peripheral macrophages, or both. Moreover, the effects of peripherally administered AE1-329 on hippocampal inflammation could be due to anti-inflammatory effects of microglial EP4, macrophage EP4, or both.

To address specifically whether peripheral EP4 signaling could modulate central inflammatory processes, we used a proteomic approach and examined plasma secreted proteins from mice stimulated with LPS +/- AE1-329. Previous studies have demonstrated a very rapid induction of pro-inflammatory cytokines in response to LPS within 2-4 hours (49, 51) so we selected an early time point of 3 hours after LPS administration to test the effects of selective activation of peripheral EP4 signaling. Co-administration of AE1-329 had a significant and broad anti-inflammatory effect on plasma cytokine and chemokine levels in LPS stimulated mice (Figure 8A and B). EP4 receptor activation in LPS-treated mice significantly decreased levels of cytokines TNF α , IL-1 α , eotaxin, and chemokines MDC, MIP-1 α , MIP-1 β , MIP-1 γ , MIP-2, MCP-1, MCP-3, and MCP-5, and reduced secreted levels of myeloperoxidase; levels of IL-6 and LIF showed a trend towards decreased levels at 6 h. Finally, EP4 agonist significantly increased plasma levels of the anti-inflammatory IL-10. Thus, peripherally administered EP4 agonist blunted serum (Figure 8) as well as hippocampal inflammatory responses (Figure 6). This would suggest that peripheral-to-central innate immune responses may be modulated in a beneficial manner by selectively targeting the EP4 receptor.

DISCUSSION

COX-2 enzymatic activity and its downstream prostaglandin signaling pathways are major components of the neuroinflammatory response. Recent *in vivo* and *in vitro* studies have identified the microglial PGE₂ EP2 receptor as a major effector of injury in models of neurodegeneration where innate immune mechanisms of inflammation are a dominant pathogenic mechanism (19-22, 52) but see (53). In the present study, we sought to investigate the function of the related PGE₂ EP4 receptor that shares similar signaling properties, cellular distribution, and inducibility in response to LPS.

In BV-2 cells and primary microglia, pharmacologic activation of EP4 downregulated a large cassette of pro-inflammatory genes, including COX-2, iNOS, pro-inflammatory cytokines IL-1 β , TNF α , and IL-6. In addition, EP4 downregulated expression of gp91^{phox} of the NADPH oxidase complex, a principal generator of superoxide in inflammation. Conversely, EP4 upregulated levels of the anti-inflammatory cytokine IL-10 by microglial cells. EP4 signaling in LPS-stimulated cells was associated with increased PKA activity but decreased Akt phosphorylation, reduced IKK phosphorylation, and decreased NF-kappa nuclear translocation, providing a potential mechanism for the anti-inflammatory effect of EP4. EP4-mediated suppression of the inflammatory response to LPS was then confirmed *in vivo*, where conditional deletion of EP4 in macrophage/microglial cells resulted in persistent elevation of pro-inflammatory genes and proteins in hippocampus and increased lipid peroxidation in cerebral cortex. Conversely, peripheral administration of EP4 agonist inhibited the acute LPS inflammatory gene response in hippocampus. Examination of plasma from LPS-stimulated mice demonstrated that administration of EP4 agonist significantly decreased the serum cytokine response to LPS, effectively blunting the peripheral-to-central immune response. Although we did not investigate what the respective contributions of peripheral macrophages and brain microglia are to the EP4-mediated hippocampal inflammatory response, this can potentially be addressed in future studies using chimeric mouse strategies. Taken together, the findings in the present study demonstrate an anti-inflammatory function for the PGE₂ EP4 receptor *in vivo* in CNS innate inflammation.

Microglial activation can result in pro- or anti-inflammatory effects, the latter presumably serving to control the inflammatory response so that it is self-limited and not injurious. One anti-inflammatory mechanism is the elaboration of cytokines such as IL-10, which was observed *in vitro* in BV-2 cells and primary microglia and *in vivo* in plasma with EP4 receptor activation. A second anti-inflammatory mechanism might consist of suppression of pro-inflammatory gene expression. LPS is a potent immunogen and binds the macrophage/microglial CD14 receptor/TLR4; this in turn causes activation of mitogen-activated protein kinases and NF-kappaB that regulate transcription of a large cassette of pro-inflammatory genes including COX-2, iNOS, cytokines, chemokines, and NADPH oxidase subunits. We found that selective activation of EP4 receptor downregulated a large number of these canonical pro-inflammatory genes, including iNOS, COX-2, TNF α , IL-6, IL-1 β , and subunits of NADPH oxidase, suggesting an effect on NF-kappaB transcription of these genes.

In LPS-stimulated BV-2 cells, EP4 signaling involved both the PKA and PI3K/Akt pathways, consistent with previous observations in transfected HEK cells showing that EP4 can couple not only to G α s subunit but also to a pertussis-sensitive cAMP inhibitory protein (or G α i subunit) with subsequent activation of PI3K and its primary target Akt (42). Stimulation of microglial BV-2 cells with EP4 agonist either alone or with LPS resulted in increased PKA activity, indicating that this pathway is active in this paradigm. In addition, the anti-inflammatory effect of EP4 in LPS-treated BV-2 cells was associated with

decreased Akt phosphorylation, as evidenced by decreases in ratios of phospho-Akt/total Akt. Moreover, in the setting of LPS stimulation, EP4 activation decreased phosphorylation of IKK α / β subunits and decreased nuclear translocation of the NF-kappaB subunits p65 and p50, suggesting a possible mechanism for the reduced transcription of LPS-induced pro-inflammatory genes. Interestingly, several studies have demonstrated that phospho-Akt can activate the Ikappa B kinase complex (IKK) by phosphorylation of serines on the IKK α and IKK β subunits (43-46) but see (47). Although in this study we did not determine whether inhibition of EP4-mediated Akt-phosphorylation would abrogate its anti-inflammatory effect, this can be explored in future studies. However, as the EP4 receptor appears to signal not only through the PI3K-Akt pathway, but also through the cAMP/PKA pathway in this model, it is possible that more than one pathway is involved in its anti-inflammatory effect.

The findings of an anti-inflammatory effect of EP4 in innate immunity support previous studies in microglia stimulated with LPS, where PGE₂ reduced production of the pro-inflammatory genes IL-1 β (54) and iNOS (55), and in macrophages where PGE₂ signaling via the EP4 receptor decreased levels of MIP-1 β (56), TNF α and IL-12 (57). The net effect of PGE₂ on microglia will depend on several things, including the dynamics of expression of EP receptors on microglial cells, the affinity of the EP receptors for PGE₂, the time course of receptor activation and desensitization, the specific downstream signaling pathways for each receptor, and the constitutive activity of the EP receptors. A number of these variables have been examined in simple in vitro systems- for example the affinity of the EP4 receptor for PGE₂ is higher than for EP2, the desensitization kinetics of EP4 are rapid in comparison to EP2, and the longer carboxy tail of EP4 is associated with a complex downstream signaling involving not only PKA and PI3K signaling, but also G α and Gi signaling (39-40). Intriguingly, recent studies in peripheral macrophages demonstrate that EP4, via its EP4-interacting protein (or EPRAP) (58), reduces phosphorylation and degradation of p105/p50 and subsequent NF-kappaB activation (59).

LPS peripheral administration results in significant changes in hippocampal glial activation, neuronal and synaptic viability, and hippocampal-dependent behaviors (6, 8-11). These effects result from both direct and indirect effects of systemic LPS on hippocampal function. LPS can directly inflame brain via TLR4 signal transduction (60, 61) or activation of cerebral perivascular macrophages (62). Indirect effects are mediated via LPS-induced cytokine responses in serum, in particular via IL-6 and IL-1 β that transduce inflammatory signals via endothelial cells to brain parenchyma. Therefore, we examined the anti-inflammatory function of EP4 in vivo using the Cd11bCre recombinase that excises floxed sequences in the monocytic cell lineage, including circulating monocytes, peripheral macrophages, and brain microglia. Cd11bCre-mediated deletion of EP4 enhanced lipid peroxidation and expression of inflammatory genes in hippocampus as well as in isolated microglia from adult mice following systemic LPS administration. Significant increases were noted in levels of the pro-inflammatory cytokines TNF α , IL-6, and IL-1 β , COX-2, and subunits of the NADPH oxidase complex. These data indicate that the EP4 receptor also functions in vivo in an anti-inflammatory manner, and its deletion results in a dysregulated inflammatory response, with persistent increases in pro-inflammatory gene expression and increased inflammatory oxidative injury in brain. Indeed, gene expression studies in isolated microglia in EP4 conditional knockout mice indicate that although the initial increase of pro-inflammatory mRNAs following LPS does not differ early at 6 hours (Figure 7), the later normal resolution by 24 hours does not occur, suggesting a failure to reset the response back to basal conditions. It might be possible that EP4 is involved in silencing the neuroinflammatory response, consistent with the concept of regulatory pathways responsible for abrogating the inflammatory response (reviewed in (63)). This is relevant because the innate immune response, although initially protective in its clearance of pathogenic substances, can also be injurious because components of the innate immune response are

cytotoxic and lead to neurodegeneration. Thus EP4 may be acting as a suppressor of brain inflammation through direct effects on innate immune cells such as macrophages and brain microglia. Alternatively, it is possible that EP4 signaling may function in alternative activation macrophages/microglia, a state more associated with phagocytosis given the positive regulation of IL10; quantification of markers of alternate activation, including cytokines such as IL-4, IL-14, and TGF β and scavenger receptors such as SR-A and SR-B would be helpful in examining this.

Peripheral administration of the selective EP4 agonist AE1-329 led to significant downregulation of pro-inflammatory gene expression in hippocampus of LPS-treated mice. Examination of plasma cytokine levels in LPS-treated mice revealed a broad and significant downregulation of many pro-inflammatory cytokines and chemokines that are regulated by NF-kappaB in EP4 agonist-treated mice. Significant decreases were seen in pro-inflammatory cytokines IL-6, IL-1 α and TNF- α , and in chemokines including MCP-1, -3, -5, MIP-1 α , MIP-1 β , and MIP-2 that serve as chemoattractants for a range of inflammatory cells including neutrophils, macrophages, and lymphocytes. Conversely, EP4 agonist elicited a marked increase in the anti-inflammatory cytokine IL-10. Secreted levels of myeloperoxidase from macrophages and neutrophils were also significantly decreased. These findings suggest that peripheral anti-inflammatory effects of EP4 signaling may attenuate consequent CNS inflammation by suppressing transmission of the systemic immune response to brain. A unidirectional transmission of inflammatory injury from periphery to CNS has been demonstrated in the case of peripheral LPS administration, a model of bacterial infection or sepsis, which can result not only in hippocampal neuronal injury and behavioral changes (8) but in late-onset and selective dopaminergic neuronal loss (11). These data are also relevant to the concept of an immune peripheral-to-central connection in neurodegenerative disorders (reviewed in (64)) such as Alzheimer's disease (AD) (65), amyotrophic lateral sclerosis (ALS) (66), Parkinson's disease (PD) (67), and stroke (68) where the relationship between peripheral innate immune responses and CNS inflammation is beginning to be investigated.

Neuroinflammation results in significant neuronal injury and behavioral deficits, as exemplified by various models of neurodegeneration including PD, AD, and ALS, where the CNS innate immune response is an important component of disease progression. The enzymatic activity of COX-2 has long been associated with exacerbation of the neuroinflammatory response in brain and inhibition of COX-2 is beneficial in rodent models of neurodegenerative disease. However, studies in humans demonstrate that sustained COX-2 inhibition has deleterious effects related to the suppression of beneficial prostaglandin signaling pathways (69, 70). So far, these effects have been linked to prostaglandin-mediated effects on vascular function, specifically the vasodilatory and anti-thrombotic effects of the prostacyclin IP receptor (71). Here we identify the PGE₂ EP4 receptor as an analogous and beneficial prostaglandin receptor that plays an important role in regulating the innate neuroinflammatory response in vivo. Further studies are required to address the therapeutic potential of selectively targeting the EP4 receptor in inflammatory neurological and neurodegenerative diseases.

Supplementary Material

Refer to Web version on PubMed Central for supplementary material.

Acknowledgments

The authors thank Ms Angela Wilson and Aimee Schantz for technical assistance. The authors also would like to acknowledge the kind assistance of Saul Villeda and Jiusheng Deng.

This work was supported by the American Federation for Aging Research (KA), Department of Defense PR043148 (KA), R21AG033914(KA), RO1AG030209 (KA), Alzheimer's Association (KA), AG24011 (TJM), AG05136 (TJM).

REFERENCES

1. Nguyen MD, Julien JP, Rivest S. Innate immunity: the missing link in neuroprotection and neurodegeneration? *Nature reviews*. 2002; 3:216–227.
2. Fassbender K, Walter S, Kuhl S, Landmann R, Ishii K, Bertsch T, Stalder AK, Muehlhauser F, Liu Y, Ulmer AJ, Rivest S, Lentschat A, Gulbins E, Jucker M, Staufenbiel M, Brechtel K, Walter J, Multhaup G, Penke B, Adachi Y, Hartmann T, Beyreuther K. The LPS receptor (CD14) links innate immunity with Alzheimer's disease. *Faseb J*. 2004; 18:203–205. [PubMed: 14597556]
3. Walter S, Letiembre M, Liu Y, Heine H, Penke B, Hao W, Bode B, Manietta N, Walter J, Schulz-Schuffer W, Fassbender K. Role of the toll-like receptor 4 in neuroinflammation in Alzheimer's disease. *Cell Physiol Biochem*. 2007; 20:947–956. [PubMed: 17982277]
4. Moisse K, Strong MJ. Innate immunity in amyotrophic lateral sclerosis. *Biochim Biophys Acta*. 2006; 1762:1083–1093. [PubMed: 16624536]
5. Letiembre M, Liu Y, Walter S, Hao W, Pfander T, Wrede A, Schulz-Schaeffer W, Fassbender K. Screening of innate immune receptors in neurodegenerative diseases: A similar pattern. *Neurobiol Aging*. 2007
6. Qin L, Wu X, Block ML, Liu Y, Breese GR, Hong JS, Knapp DJ, Crews FT. Systemic LPS causes chronic neuroinflammation and progressive neurodegeneration. *Glia*. 2007; 55:453–462. [PubMed: 17203472]
7. Letiembre M, Hao W, Liu Y, Walter S, Mihaljevic I, Rivest S, Hartmann T, Fassbender K. Innate immune receptor expression in normal brain aging. *Neuroscience*. 2007; 146:248–254. [PubMed: 17293054]
8. Semmler A, Frisch C, Debeir T, Ramanathan M, Okulla T, Klockgether T, Heneka MT. Long-term cognitive impairment, neuronal loss and reduced cortical cholinergic innervation after recovery from sepsis in a rodent model. *Exp Neurol*. 2007; 204:733–740. [PubMed: 17306796]
9. Minghetti L. Role of inflammation in neurodegenerative diseases. *Current opinion in neurology*. 2005; 18:315–321. [PubMed: 15891419]
10. McGeer PL, McGeer EG. Inflammation and the degenerative diseases of aging. *Ann N Y Acad Sci*. 2004; 1035:104–116. [PubMed: 15681803]
11. Liu Y, Qin L, Wilson B, Wu X, Qian L, Granholm AC, Crews FT, Hong JS. Endotoxin induces a delayed loss of TH-IR neurons in substantia nigra and motor behavioral deficits. *Neurotoxicology*. 2008; 29:864–870. [PubMed: 18471886]
12. Minghetti L. Cyclooxygenase-2 (COX-2) in inflammatory and degenerative brain diseases. *J Neuropathol Exp Neurol*. 2004; 63:901–910. [PubMed: 15453089]
13. Hewett SJ, Bell SC, Hewett JA. Contributions of cyclooxygenase-2 to neuroplasticity and neuropathology of the central nervous system. *Pharmacology & therapeutics*. 2006; 112:335–357. [PubMed: 16750270]
14. Heneka MT, O'Banion MK. Inflammatory processes in Alzheimer's disease. *Journal of neuroimmunology*. 2007; 184:69–91. [PubMed: 17222916]
15. Hein AM, O'Banion MK. Neuroinflammation and Memory: The Role of Prostaglandins. *Mol Neurobiol*. 2009
16. Breyer RM, Bagdassarian CK, Myers SA, Breyer MD. Prostanoid receptors: subtypes and signaling. *Annu Rev Pharmacol Toxicol*. 2001; 41:661–690. [PubMed: 11264472]
17. Hata AN, Breyer RM. Pharmacology and signaling of prostaglandin receptors: multiple roles in inflammation and immune modulation. *Pharmacology & therapeutics*. 2004; 103:147–166. [PubMed: 15369681]
18. Andreasson K. Emerging roles of PGE2 receptors in models of neurological disease. *Prostaglandins Other Lipid Mediat*. 2009

19. Montine TJ, Milatovic D, Gupta RC, Valyi-Nagy T, Morrow JD, Breyer RM. Neuronal oxidative damage from activated innate immunity is EP2 receptor-dependent. *J Neurochem.* 2002; 83:463–470. [PubMed: 12423256]
20. Liang X, Wang Q, Hand T, Wu L, Breyer RM, Montine TJ, Andreasson K. Deletion of the prostaglandin E2 EP2 receptor reduces oxidative damage and amyloid burden in a model of Alzheimer's disease. *J Neurosci.* 2005; 25:10180–10187. [PubMed: 16267225]
21. Liang X, Wang Q, Shi J, Lokteva L, Breyer RM, Montine TJ, Andreasson K. The prostaglandin E2 EP2 receptor accelerates disease progression and inflammation in a model of amyotrophic lateral sclerosis. *Ann Neurol.* 2008; 64:304–314. [PubMed: 18825663]
22. Jin J, Shie FS, Liu J, Wang Y, Davis J, Schantz AM, Montine KS, Montine TJ, Zhang J. Prostaglandin E2 receptor subtype 2 (EP2) regulates microglial activation and associated neurotoxicity induced by aggregated alpha-synuclein. *J Neuroinflammation.* 2007; 4:2. [PubMed: 17204153]
23. Ahmad AS, Zhuang H, Echeverria V, Dore S. Stimulation of prostaglandin EP2 receptors prevents NMDA-induced excitotoxicity. *Journal of neurotrauma.* 2006; 23:1895–1903. [PubMed: 17184197]
24. Bilak M, Wu L, Wang Q, Haughey N, Conant K, St Hillaire C, Andreasson K. PGE2 receptors rescue motor neurons in a model of amyotrophic lateral sclerosis. *Ann Neurol.* 2004; 56:240–248. [PubMed: 15293276]
25. Carrasco E, Werner P, Casper D. Prostaglandin receptor EP2 protects dopaminergic neurons against 6-OHDA-mediated low oxidative stress. *Neuroscience letters.* 2008; 441:44–49. [PubMed: 18597941]
26. Li J, Liang X, Wang Q, Breyer RM, McCullough L, Andreasson K. Misoprostol, an anti-ulcer agent and PGE(2) receptor agonist, protects against cerebral ischemia. *Neuroscience letters.* 2008; 438:210–215. [PubMed: 18472336]
27. Liu D, Wu L, Breyer R, Mattson MP, Andreasson K. Neuroprotection by the PGE2 EP2 receptor in permanent focal cerebral ischemia. *Ann Neurol.* 2005; 57:758–761. [PubMed: 15852374]
28. McCullough L, Wu L, Haughey N, Liang X, Hand T, Wang Q, Breyer RM, Andreasson K. Neuroprotective function of the PGE2 EP2 receptor in cerebral ischemia. *J Neurosci.* 2004; 24:257–268. [PubMed: 14715958]
29. Zhang J, Rivest S. Distribution, regulation and colocalization of the genes encoding the EP2- and EP4-PGE2 receptors in the rat brain and neuronal responses to systemic inflammation. *Eur J Neurosci.* 1999; 11:2651–2668. [PubMed: 10457163]
30. Suzawa T, Miyaura C, Inada M, Maruyama T, Sugimoto Y, Ushikubi F, Ichikawa A, Narumiya S, Suda T. The role of prostaglandin E receptor subtypes (EP1, EP2, EP3, and EP4) in bone resorption: an analysis using specific agonists for the respective EPs. *Endocrinology.* 2000; 141:1554–1559. [PubMed: 10746663]
31. Shibuya I, Setiadji SV, Ibrahim N, Harayama N, Maruyama T, Ueta Y, Yamashita H. Involvement of postsynaptic EP4 and presynaptic EP3 receptors in actions of prostaglandin E2 in rat supraoptic neurones. *Journal of neuroendocrinology.* 2002; 14:64–72. [PubMed: 11903814]
32. Schneider A, Guan Y, Zhang Y, Magnuson MA, Pettepher C, Loftin CD, Langenbach R, Breyer RM, Breyer MD. Generation of a conditional allele of the mouse prostaglandin EP4 receptor. *Genesis.* 2004; 40:7–14. [PubMed: 15354288]
33. Boillee S, Yamanaka K, Lobsiger CS, Copeland NG, Jenkins NA, Kassiotis G, Kollias G, Cleveland DW. Onset and progression in inherited ALS determined by motor neurons and microglia. *Science.* 2006; 312:1389–1392. [PubMed: 16741123]
34. Nagamatsu T, Imai H, Yokoi M, Nishiyama T, Hirasawa Y, Nagao T, Suzuki Y. Protective effect of prostaglandin EP4-receptor agonist on anti-glomerular basement membrane antibody-associated nephritis. *J Pharmacol Sci.* 2006; 102:182–188. [PubMed: 17031072]
35. Cardona AE, Huang D, Sasse ME, Ransohoff RM. Isolation of murine microglial cells for RNA analysis or flow cytometry. *Nature protocols.* 2006; 1:1947–1951.
36. de Haas AH, Boddeke HW, Brouwer N, Biber K. Optimized isolation enables ex vivo analysis of microglia from various central nervous system regions. *Glia.* 2007; 55:1374–1384. [PubMed: 17661344]

37. Blasi E, Barluzzi R, Bocchini V, Mazzolla R, Bistoni F. Immortalization of murine microglial cells by a v-raf/v-myc carrying retrovirus. *Journal of neuroimmunology*. 1990; 27:229–237. [PubMed: 2110186]
38. Bhattacharya M, Peri K, Ribeiro-da-Silva A, Almazan G, Shichi H, Hou X, Varma DR, Chemtob S. Localization of functional prostaglandin E2 receptors EP3 and EP4 in the nuclear envelope. *J Biol Chem*. 1999; 274:15719–15724. [PubMed: 10336471]
39. Bhattacharya M, Peri KG, Almazan G, Ribeiro-da-Silva A, Shichi H, Durocher Y, Abramovitz M, Hou X, Varma DR, Chemtob S. Nuclear localization of prostaglandin E2 receptors. *Proc Natl Acad Sci U S A*. 1998; 95:15792–15797. [PubMed: 9861049]
40. Gobeil F Jr, Vazquez-Tello A, Marrache AM, Bhattacharya M, Checchin D, Bkaily G, Lachapelle P, Ribeiro-Da-Silva A, Chemtob S. Nuclear prostaglandin signaling system: biogenesis and actions via heptahelical receptors. *Can J Physiol Pharmacol*. 2003; 81:196–204. [PubMed: 12710534]
41. Fujino H, West KA, Regan JW. Phosphorylation of glycogen synthase kinase-3 and stimulation of T-cell factor signaling following activation of EP2 and EP4 prostanoid receptors by prostaglandin E2. *J Biol Chem*. 2002; 277:2614–2619. [PubMed: 11706038]
42. Fujino H, Regan JW. EP(4) prostanoid receptor coupling to a pertussis toxin-sensitive inhibitory G protein. *Mol Pharmacol*. 2006; 69:5–10. [PubMed: 16204467]
43. Bai D, Ueno L, Vogt PK. Akt-mediated regulation of NFkappaB and the essentialness of NFkappaB for the oncogenicity of PI3K and Akt. *Int J Cancer*. 2009
44. Barre B, Perkins ND. A cell cycle regulatory network controlling NF-kappaB subunit activity and function. *Embo J*. 2007; 26:4841–4855. [PubMed: 17962807]
45. Gustin JA, Maehama T, Dixon JE, Donner DB. The PTEN tumor suppressor protein inhibits tumor necrosis factor-induced nuclear factor kappa B activity. *J Biol Chem*. 2001; 276:27740–27744. [PubMed: 11356844]
46. Ozes ON, Mayo LD, Gustin JA, Pfeffer SR, Pfeffer LM, Donner DB. NF-kappaB activation by tumour necrosis factor requires the Akt serine-threonine kinase. *Nature*. 1999; 401:82–85. [PubMed: 10485710]
47. Delhase M, Li N, Karin M. Kinase regulation in inflammatory response. *Nature*. 2000; 406:367–368. [PubMed: 10935625]
48. DiDonato JA, Hayakawa M, Rothwarf DM, Zandi E, Karin M. A cytokine-responsive IkappaB kinase that activates the transcription factor NF-kappaB. *Nature*. 1997; 388:548–554. [PubMed: 9252186]
49. Lund S, Christensen KV, Hedtjarn M, Mortensen AL, Hagberg H, Falsig J, Hasseldam H, Schratzenholz A, Porzgen P, Leist M. The dynamics of the LPS triggered inflammatory response of murine microglia under different culture and in vivo conditions. *Journal of neuroimmunology*. 2006; 180:71–87. [PubMed: 16996144]
50. Laye S, Parnet P, Goujon E, Dantzer R. Peripheral administration of lipopolysaccharide induces the expression of cytokine transcripts in the brain and pituitary of mice. *Brain Res Mol Brain Res*. 1994; 27:157–162. [PubMed: 7877446]
51. Rosenberger CM, Scott MG, Gold MR, Hancock RE, Finlay BB. Salmonella typhimurium infection and lipopolysaccharide stimulation induce similar changes in macrophage gene expression. *J Immunol*. 2000; 164:5894–5904. [PubMed: 10820271]
52. Shie FS, Montine KS, Breyer RM, Montine TJ. Microglial EP2 is critical to neurotoxicity from activated cerebral innate immunity. *Glia*. 2005; 52:70–77. [PubMed: 15920732]
53. Caggiano AO, Kraig RP. Prostaglandin E receptor subtypes in cultured rat microglia and their role in reducing lipopolysaccharide-induced interleukin-1 β production. *J Neurochem*. 1999; 72:565–575. [PubMed: 9930728]
54. Caggiano AO, Kraig RP. Prostaglandin E2 and 4-aminopyridine prevent the lipopolysaccharide-induced outwardly rectifying potassium current and interleukin-1beta production in cultured rat microglia. *J Neurochem*. 1998; 70:2357–2368. [PubMed: 9603200]
55. Minghetti L, Nicolini A, Polazzi E, Creminon C, Maclouf J, Levi G. Prostaglandin E2 downregulates inducible nitric oxide synthase expression in microglia by increasing cAMP levels. *Adv Exp Med Biol*. 1997; 433:181–184. [PubMed: 9561130]

56. Takayama K, Garcia-Cardena G, Sukhova GK, Comander J, Gimbrone MA Jr, Libby P. Prostaglandin E2 suppresses chemokine production in human macrophages through the EP4 receptor. *J Biol Chem.* 2002; 277:44147–44154. [PubMed: 12215436]
57. Nataraj C, Thomas DW, Tilley SL, Nguyen MT, Mannon R, Koller BH, Coffman TM. Receptors for prostaglandin E(2) that regulate cellular immune responses in the mouse. *J Clin Invest.* 2001; 108:1229–1235. [PubMed: 11602631]
58. Takayama K, Sukhova GK, Chin MT, Libby P. A novel prostaglandin E receptor 4-associated protein participates in antiinflammatory signaling. *Circ Res.* 2006; 98:499–504. [PubMed: 16424369]
59. Minami M, Shimizu K, Okamoto Y, Folco E, Ilasaca ML, Feinberg MW, Aikawa M, Libby P. Prostaglandin E receptor type 4-associated protein interacts directly with NF-kappaB1 and attenuates macrophage activation. *J Biol Chem.* 2008; 283:9692–9703. [PubMed: 18270204]
60. Rivest S. Molecular insights on the cerebral innate immune system. *Brain, behavior, and immunity.* 2003; 17:13–19.
61. Chakravarty S, Herkenham M. Toll-like receptor 4 on nonhematopoietic cells sustains CNS inflammation during endotoxemia, independent of systemic cytokines. *J Neurosci.* 2005; 25:1788–1796. [PubMed: 15716415]
62. Williams K, Alvarez X, Lackner AA. Central nervous system perivascular cells are immunoregulatory cells that connect the CNS with the peripheral immune system. *Glia.* 2001; 36:156–164. [PubMed: 11596124]
63. Griffiths M, Neal JW, Gasque P. Innate immunity and protective neuroinflammation: new emphasis on the role of neuroimmune regulatory proteins. *International review of neurobiology.* 2007; 82:29–55. [PubMed: 17678954]
64. Teeling JL, Perry VH. Systemic infection and inflammation in acute CNS injury and chronic neurodegeneration: underlying mechanisms. *Neuroscience.* 2009; 158:1062–1073. [PubMed: 18706982]
65. Ray S, Britschgi M, Herbert C, Takeda-Uchimura Y, Boxer A, Blenow K, Friedman LF, Galasko DR, Jutel M, Karydas A, Kaye JA, Leszek J, Miller BL, Minthon L, Quinn JF, Rabinovici GD, Robinson WH, Sabbagh MN, So YT, Sparks DL, Tabaton M, Tinklenberg J, Yesavage JA, Tibshirani R, Wyss-Coray T. Classification and prediction of clinical Alzheimer's diagnosis based on plasma signaling proteins. *Nature medicine.* 2007; 13:1359–1362.
66. Keizman D, Rogowski O, Berliner S, Ish-Shalom M, Maimon N, Nefussy B, Artamonov I, Drory VE. Low-grade systemic inflammation in patients with amyotrophic lateral sclerosis. *Acta Neurol Scand.* 2008
67. Reale M, Iarlori C, Thomas A, Gambi D, Perfetti B, Di Nicola M, Onofri M. Peripheral cytokines profile in Parkinson's disease. *Brain, behavior, and immunity.* 2009; 23:55–63.
68. Wang Q, Tang XN, Yenari MA. The inflammatory response in stroke. *Journal of neuroimmunology.* 2007; 184:53–68. [PubMed: 17188755]
69. Cheng Y, Austin SC, Rocca B, Koller BH, Coffman TM, Grosser T, Lawson JA, FitzGerald GA. Role of prostacyclin in the cardiovascular response to thromboxane A2. *Science.* 2002; 296:539–541. [PubMed: 11964481]
70. Funk CD, FitzGerald GA. COX-2 inhibitors and cardiovascular risk. *J Cardiovasc Pharmacol.* 2007; 50:470–479. [PubMed: 18030055]
71. Egan KM, Lawson JA, Fries S, Koller B, Rader DJ, Smyth EM, Fitzgerald GA. COX-2-derived prostacyclin confers atheroprotection on female mice. *Science.* 2004; 306:1954–1957. [PubMed: 15550624]

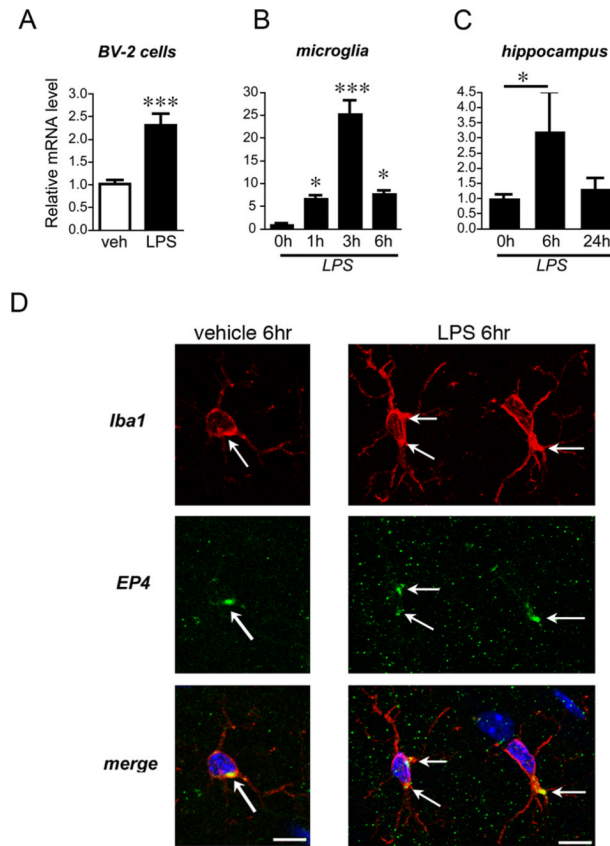


Figure 1. EP4 receptor expression is dynamically regulated in BV-2 microglial-like cells, in primary microglia, and in hippocampus in response to LPS stimulation

(A) Murine BV-2 cells were stimulated with vehicle or LPS (10ng/ml), and EP4 mRNA was measured at 6h by qPCR ($p < 0.001$; $n = 3$ per condition). (B) EP4 mRNA is also dynamically regulated in rat primary microglia derived from cerebral cortex and hippocampus (ANOVA $p < 0.001$; by post hoc analysis $p < 0.05$ at 1h, $p < 0.001$ at 3h, and $p < 0.05$ at 6h; $n = 3$ per condition). (C) EP4 mRNA is upregulated at 6h in mouse hippocampus and returns to baseline by 24h after peripheral administration of LPS (5 mg/kg IP; $n = 3-6$ per group; $p < 0.05$). (D) Confocal 400X imaging is shown of microglial cells in the hilar region of hippocampus from vehicle-treated and LPS-treated mice (5 mg/kg IP at 6 hours after stimulation). EP4 signal is localized in Iba1 positive microglia (arrows) in a punctate perinuclear distribution in both vehicle and LPS treated mice (scale bar = 10 microns).

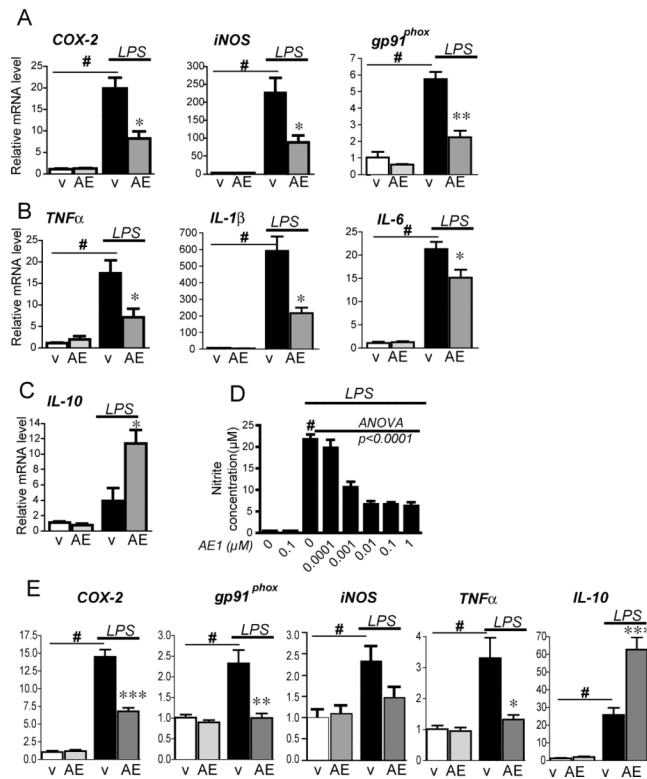


Figure 2. EP4 signaling suppresses pro-inflammatory gene transcription in BV-2 cells and primary microglia stimulated with LPS

BV-2 cells (A-D) and cerebral cortical microglia (E) were stimulated with LPS (10 ng/ml) or PBS +/- the EP4 agonist AE1-329 (1 μ M) or vehicle. (A) qPCR of COX-2, iNOS, and gp91^{phox} in BV-2 cells at 6h shows a significant increase with LPS treatment in vehicle (v) treated groups (# p <0.001) but a significant decrease with co-administration of AE1-329 (AE; * p <0.05, ** p <0.01; n = 3 per condition). (B) Expression in BV-2 cells of pro-inflammatory cytokines TNF α , IL1 β , and IL-6 is significantly induced with LPS (# p <0.001) but decreased with co-stimulation of EP4 receptor agonist (* p <0.05). (C) The anti-inflammatory cytokine IL-10 is upregulated with EP4 receptor stimulation (p <0.05). (D) LPS-induced increase in nitrite concentration in BV-2 cells is decreased in a dose-dependent manner with AE1-329 (0-1 μ M) at 24 hours (# p <0.001 vehicle vs LPS alone; dose response for AE1-329 ANOVA p <0.0001; post hoc analysis p <0.001 for 0.001, 0.01, 0.1, and 1 μ M, n =5 per condition). (E) Primary microglia were stimulated +/- LPS +/- EP4 agonist AE1-329 (100nM) and harvested at 3 hours. qPCR demonstrates a reduced level of iNOS as well as significant reductions of COX-2, TNF- α , and gp91^{phox} and upregulation of IL-10 in LPS-treated microglia with EP4 receptor agonist (# p <0.01-0.001 for vehicle vs LPS; * p <0.05, *** p <0.001 for LPS vs LPS+AE1-329; n =6 per condition).

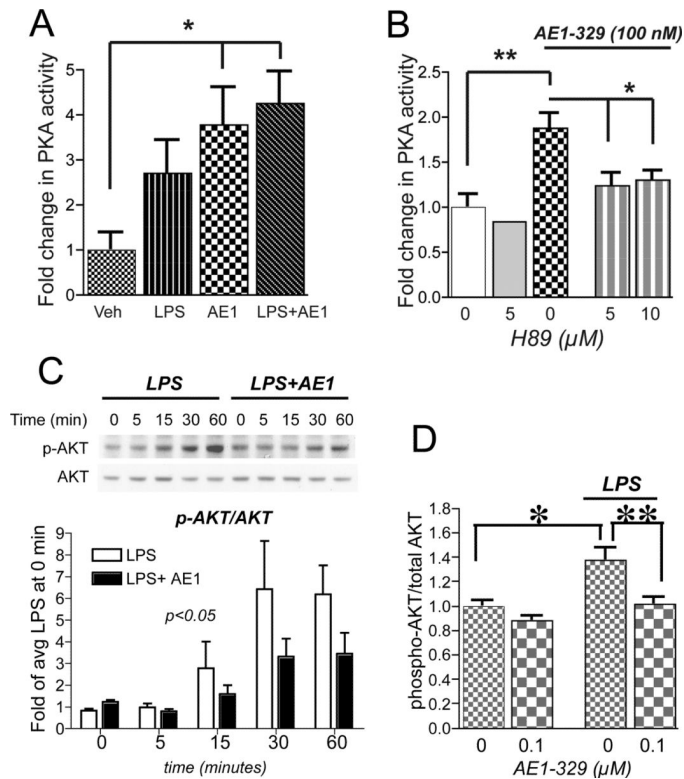


Figure 3. EP4 receptor activation in BV-2 cells increases PKA activity and reduces LPS-induced phosphorylation of Akt

(A) PKA activity assay of BV-2 cells stimulated with LPS (100 ng/ml), AE1-329 (100 nM), or both shows significant increases with AE1-329 and LPS+AE1-329 (* $p < 0.05$; $n = 5$ samples per condition). (B) Inhibition of PKA with H89 at 5 μ M and 10 μ M reverses AE1-329-mediated increase in PKA activity (* $p < 0.05$ and ** $p < 0.01$). (C) Representative quantitative Western analysis of p-Akt and total Akt shows an increase in p-Akt with LPS (100 ng/ml) treatment that is reduced with stimulation with EP4 agonist AE1-329 (100 nM). BV-2 cells were treated with LPS +/- AE1-329 or vehicle and harvested at time points of 5, 15, 30, and 60 minutes; cell lysates were immunoblotted for phosphorylated Ser473 Akt (p-Akt) and total Akt. The average densitometry from three experiments is shown in the lower panel. p-Akt/Akt values have been normalized to the average signal at time=0 minutes of LPS and LPS+AE1 values. There was a significant effect of AE1-329 treatment [$F(1,4) = 4.589$, $p < 0.05$] and of time [$F(1,4) = 7.72$, $p < 0.001$]. Densitometric measurements of effects of vehicle vs AE1-329 alone did not show differences (data not shown). (D) ELISA of phospho-Thr308 Akt and total Akt at 60 minutes after stimulation with LPS +/- AE1-329 shows a significant increase in p-Akt/Akt levels with LPS stimulation, which is reversed with co-administration of 100 nM AE1-329 (* $p < 0.05$; ** $p < 0.01$; $n = 6$ per condition).

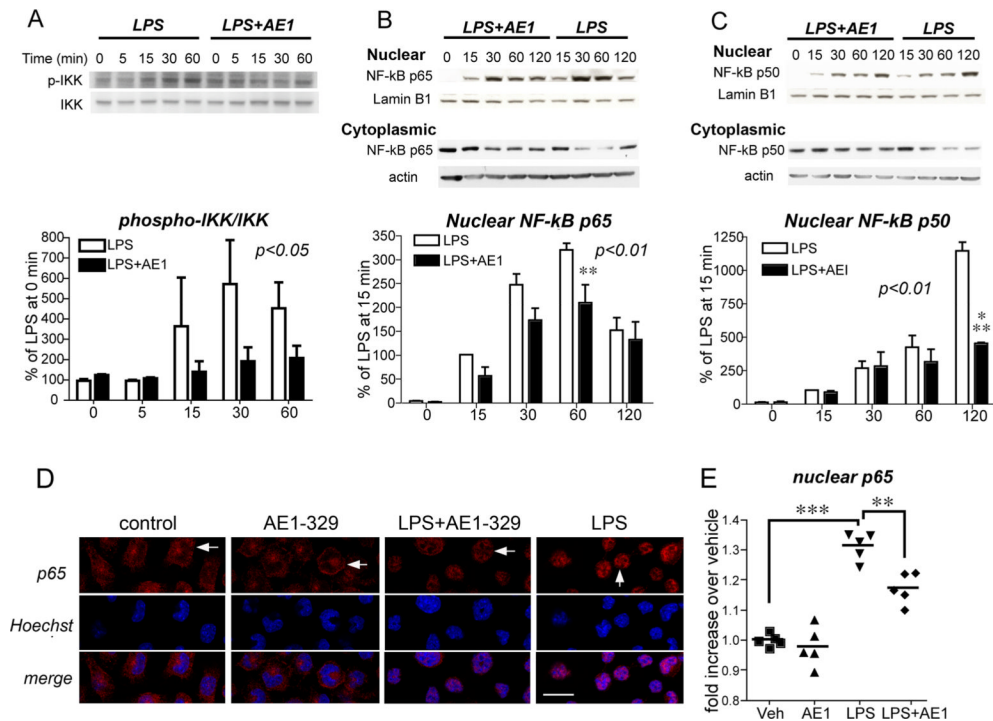


Figure 4. EP4 receptor activation in BV-2 cells reduces phosphorylation of IKK and nuclear translocation of NF- κ B subunits p65 and p50

(A) Representative quantitative Western analysis of phospho-IKK (p-IKK) and total IKK and densitometric average of three experiments demonstrates an increase in phospho-IKK with LPS stimulation (100 ng/ml) that is significantly attenuated with co-activation of the EP4 receptor (AE1, 100nM; [F(1,4)=4.709, $p < 0.05$] for effect of AE1-329). Densitometric measurements are represented as ratios of p-IKK/IKK and are normalized to time=0 minutes for LPS and LPS+AE1. (B and C) Representative quantitative Western analyses are shown for NF- κ B p65 (B) and NF- κ B p50 (C) nuclear translocation and cytoplasmic levels in BV-2 cells treated with LPS +/- AE1-329. NF- κ B subunit signals were normalized to the nuclear marker lamin B1. Densitometry measurements for nuclear levels of p65 and p50 represent averages of three experiments in which values for individual time points were normalized to the 15 minute vehicle time point. There was a significant effect of AE1-329 treatment for both p65 ([F(1,4)=11.13, $p < 0.01$]) and p50 ([F(1,4)=11.88, $p < 0.01$]) nuclear translocation; there was a significant effect of time for both p65 and p50 [F(1,4)=42.7, $p < 0.001$] and [F(1,4)=27.06, $p < 0.001$], respectively. Maximal attenuation of LPS-dependent nuclear translocation is evident by 60 minutes for NF- κ B p65 (** $p < 0.01$) and by 120 minutes for p50 (** $p < 0.001$) with activation of the EP4 receptor. (D) Nuclear translocation of NF- κ B p65 was quantified in BV-2 cells 60 minutes after stimulation with either LPS (100 ng/ml) or PBS +/- AE1-329 (100 nM) or vehicle. Cells were immunostained for NF- κ B p65 and nuclei were counterstained with Hoechst and examined at 400X with confocal microscopy (scale bar=8 microns). Immunofluorescent staining of p65 in control, AE1-329, and LPS +AE1-329 nuclei (top row in red) demonstrates more diffuse and lighter staining (white horizontal arrows), in contrast to the dense nuclear staining in LPS alone (white vertical arrow). (E) Quantification of immunofluorescent nuclear signal intensity of p65 was carried out in BV-2 cells treated with veh, AE1-329, LPS, and LPS+AE1-329. Five fields per condition were measured, representing >100 cells per field (see Methods). There was a significant increase in nuclear levels of p65 at one hour following LPS stimulation as compared to vehicle alone (** $p < 0.001$), and this increase was significantly attenuated with co-stimulation of the EP4 receptor (** $p < 0.01$).

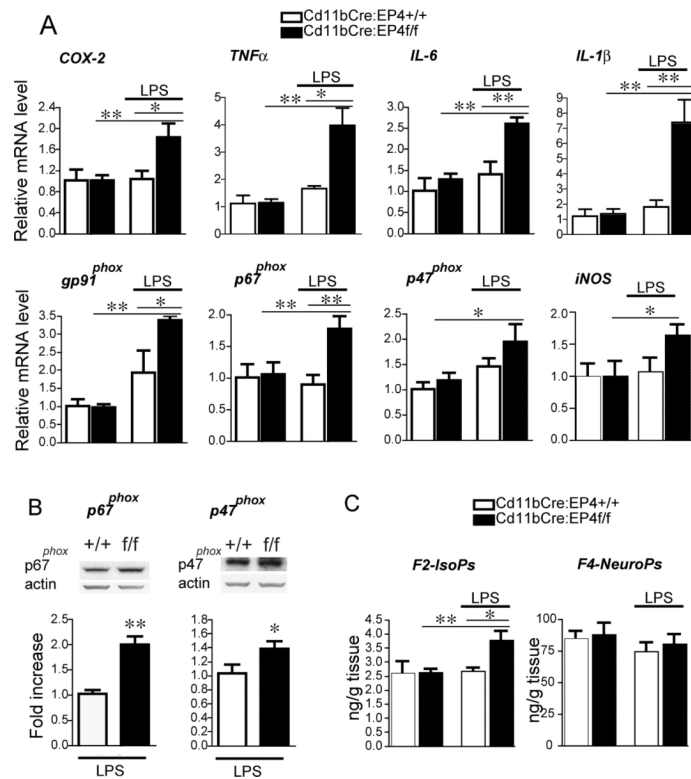


Figure 5. Cd11bCre conditional deletion of EP4 results in increased pro-inflammatory gene expression and increased lipid peroxidation in brain

Hippocampal mRNA and protein were isolated from Cd11bCre:EP4+/+ and Cd11bCre:EP4f/f male mice 24h after peripheral stimulation with LPS (5mg/kg i.p.). (A) In Cd11bCre:EP4f/f mice qPCR demonstrates increased expression of COX-2, TNF α , IL-6, IL-1 β , and NADPH oxidase subunits p47^{phox}, p67^{phox}, gp91^{phox}, and iNOS 24 hours after peripheral LPS stimulation (* p < 0.05; **p < 0.01; n = 4–7 male mice per group). (B) Representative quantitative Western analyses and densitometry of p47^{phox} and p67^{phox} in LPS treated Cd11bCre:EP4+/+ versus Cd11bCre:EP4f/f mice (n=4-5 per genotype, *p < 0.05, **p < 0.01). There were no differences between genotypes treated with vehicle (data not shown). (C) Gas chromatography mass spectrophotometric (GCMS) quantification of lipid peroxidation in cerebral cortical lysates demonstrates a significant increase in F2-isoprostanes (isoPs) in Cd11b: EP4f/f mice 24h after LPS as compared to control Cd11bCre:EP4+/+ mice treated with LPS (n = 4-7 per genotype; *p < 0.05).

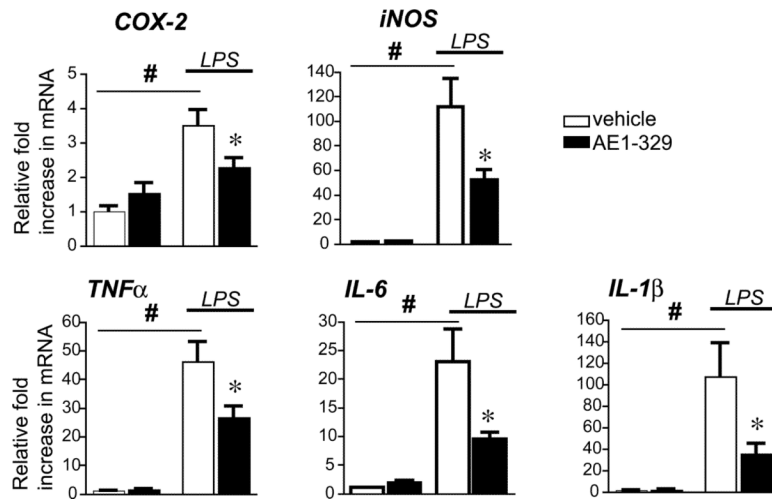


Figure 6. Systemic administration of EP4 agonist decreases LPS-induced hippocampal pro-inflammatory gene response

Mice were pretreated with AE1-329 (300 μ g/kg, s.c.) for 30 min before injection of LPS (5mg/kg, i.p.) and hippocampal RNA was isolated at 6 hours after LPS. (A) Pro-inflammatory COX-2 and iNOS are strongly induced 6h after systemic LPS administration, while administration of the selective EP4 agonist AE1-329 blunts induction. (B) Induction of cytokines TNF α , IL-6, and IL-1 β are also decreased with administration of AE1-329 (n=7-8 per group of 3 month male C57B6 mice; # p<0.001 vehicle vs LPS; *p<0.05 LPS/veh vs LPS/AE1-329).

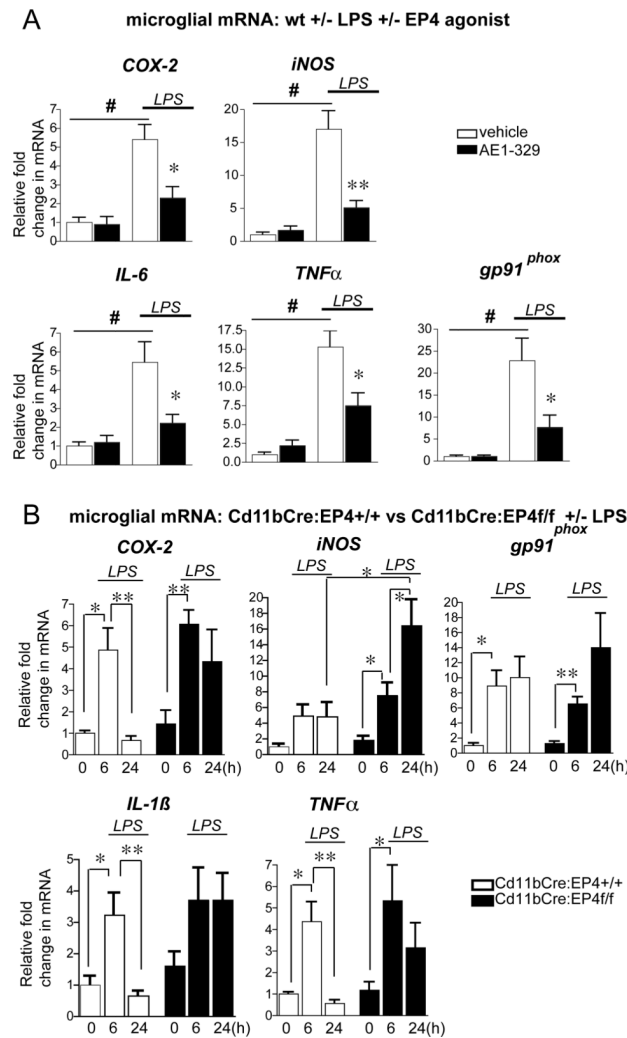


Figure 7. EP4 receptor regulates inflammatory gene expression in microglia isolated from adult mouse brain

Microglia were isolated by density gradient centrifugation from 2-3 mo C57B7 male mice administered saline or LPS +/- EP4 agonist (AE1-329 0.3mg/kg) or vehicle (A), and from 2-3 mo Cd11bCre:EP4+/+ and Cd11bCre:EP4f/f mice 6 hours and 24 hours after LPS (B). (A) Significant increases in microglial expression of COX-2, iNOS, IL-6, TNF- α , and gp91^{phox} were observed in wild type mice in response to LPS, but these increases were significantly blunted with co-treatment with EP4 agonist (#p<0.01; *p<0.05; **p<0.01; n=6-8 mice per group). (B) Proinflammatory gene expression is elevated in Cd11bCre:EP4+/+ and Cd11bCre:EP4f/f microglia at 6 hours after LPS; however, increased gene expression persists at 24h in microglia isolated from Cd11bCre:EP4f/f mice as compared to Cd11bCre:EP4+/+ control mice. Gene expression does not return to basal levels for COX-2, IL-1 β , and TNF- α at 24h in Cd11bCre:EP4f/f microglia, and is significantly increased beyond the 6 hour level for iNOS at this late time point (*p<0.05; **p<0.01; n=4-8 per group).

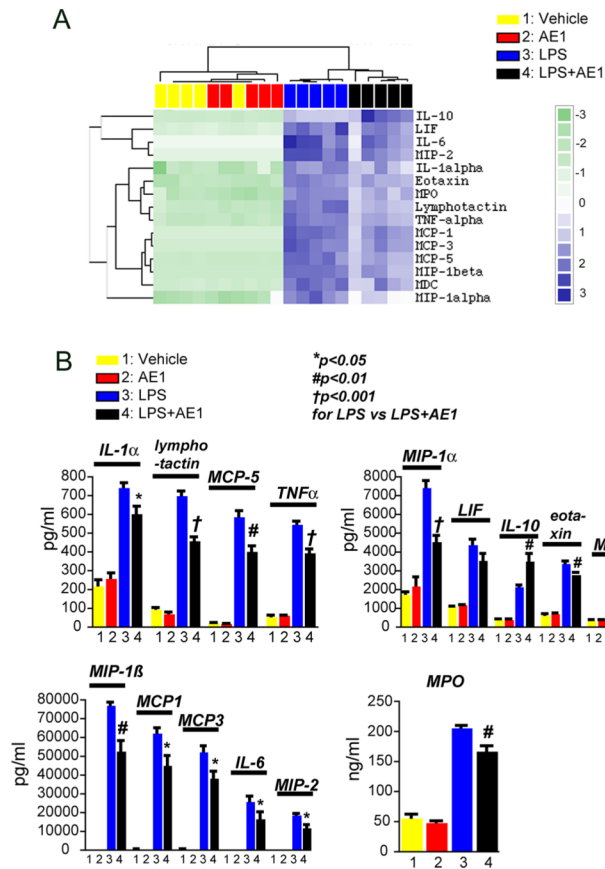


Figure 8. Peripheral administration of EP4 reduces LPS-mediated inflammatory response in plasma

Plasma was collected and analyzed at 3 hours after co-administration of PBS or LPS (5mg/kg, i.p.) +/- vehicle or AE1-329 (300 μ g/kg, s.c.). (A) Cluster analysis of regulated cytokines and myeloperoxidase (MPO) following peripheral PBS or LPS administration +/- AE1-329. (B) Absolute concentrations of regulated cytokines (pg/ml) and MPO (ng/ml) are decreased with AE1-329 administration.